How to cite: *Angew. Chem. Int. Ed.* **2024**, *63*, e202404727
doi.org/10.1002/anie.202404727

Electron Transfer | Hot Paper

Symmetric Electron Transfer Coordinates are Intrinsic to Bridged Systems: An ab Initio Treatment of the Creutz–Taube Ion

Adam Šrut, Benjamin J. Lear, and Vera Krewald**

Abstract: A long-standing question in electron transfer research concerns the number and identity of collective nuclear motions that drive electron transfer or localisation. It is well established that these nuclear motions are commonly gathered into a so-called electron transfer coordinate. In this theoretical study, we demonstrate that both anti-symmetric and symmetric vibrational motions are intrinsic to bridged systems, and that both are required to explain the characteristic shape of their intervalence charge transfer bands. Using the properties of a two-state Marcus–Hush model, we identify and quantify these two coordinates as linear combinations of normal modes from ab initio calculations. This quantification gives access to the potential coupling, reorganization energy and curvature of the potential energy surfaces involved in electron transfer, independent of any prior assumptions about the system of interest. We showcase these claims with the Creutz–Taube ion, a prototypical Class III mixed valence complex. We find that the symmetric dimension is responsible for the asymmetric band shape, and trace this back to the offset of the ground and excited state potentials in this dimension. The significance of the symmetric dimension originates from geometry dependent coupling, which in turn is a natural consequence of the well-established superexchange mechanism. The conceptual connection between the symmetric and anti-symmetric motions and the superexchange mechanism appears as a general result for bridged systems.

Introduction

Electron redistribution is at the core of every chemical transformation. For instance, electron transfer takes place in intermolecular redox events during catalysis, along enzymatic charge transport chains, or as intramolecular events in some mixed-valent compounds. Electron redistribution is associated with a change in nuclear configuration, and models are needed to describe, rationalize and predict these changes.

The simplest model might treat the transfer of a single electron between two states, each associated with the electron occupying one of two redox sites. The central model for electron transfer (ET), Marcus–Hush theory (an extension of the Marcus theory of electron transfer and their rates for strongly coupled systems, see Figure 1c),[1,2] covers this scenario. A complete model would identify the specific nuclear motions associated with ET, mapping out the relevant electronic states along these ET coordinates. It would also handle coupling between these states, which changes the observables and properties of the system. Therefore, a complete model would explain the experimental behavior of systems undergoing electron transfer. Of course, to validate any theoretical model, one needs a suitable reference compound which encompasses many or all of the testable aspects of the model.

The Creutz–Taube ion[3] (CTI, (μ-pyrazine)[$Ru^{II/III}$-$(NH_3)_5$]$_2^{5+}$) was the first molecule purposefully synthesized to study the transfer of single electrons,[4–9] and has served as a benchmark for theoretical models[10–12] and quantum chemical calculations[13–18] ever since. Its mixed valence state is stabilized relative to disproportionation by strong coupling between the metal centers. This strong coupling between the metal centers and the intramolecular nature of the ET pathway together mean that the nuclear rearrangements associated with ET will be dominated by those of the complex, simplifying what must be considered in applying a model.

The CTI was found to have an intervalence charge transfer (IVCT) absorption band in the near infra-red region, Figure 1a.[3] Its position and shape have long been used as the main tool to better understand the electronic nature of the CTI, specifically its degree of localization or delocalization.[6,7] While it is firmly assigned as a Class III system (i.e. it has a delocalized electronic structure in the framework introduced by Robin and Day),[19] detailed discussions have also established that it must lie near the Class II/III borderline,[20] meaning that it possesses properties of both localized and delocalized electronic structures.

[*] A. Šrut, Prof. Dr. V. Krewald
TU Darmstadt, Department of Chemistry, Quantum Chemistry, Peter-Grünberg-Straße 4, 64287 Darmstadt, Germany
E-mail: vera.krewald@tu-darmstadt.de
Prof. B. J. Lear
The Pennsylvania State University, Department of Chemistry, University Park, PA 16802, Pennsylvania, USA
E-mail: bul14@psu.edu

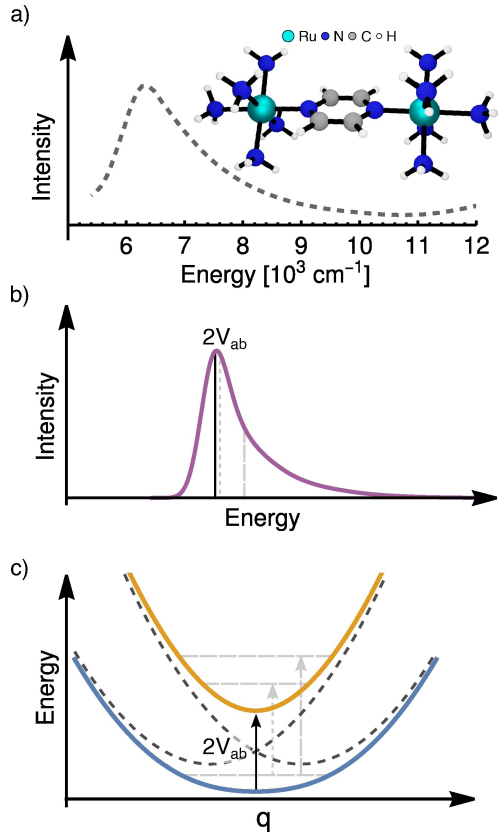

Figure 1. a) Experimental spectrum of the Creutz–Taube ion (structure shown as an inset), adapted from Ref. [3] with permission. b) Simulated IVCT band of a Class III system using the nuclear ensemble approach presented in Ref. [25]. Gray dashed lines schematically represent vibronic transitions. c) Marcus–Hush model depicting a strongly coupled (Class III) system; q denotes the electron transfer coordinate. Adiabatic potential energy curves are depicted by orange and blue solid lines. Diabatic surfaces are indicated by dashed black lines. V_{ab} is the potential coupling between the diabatic states. Vibronic transitions are depicted with gray dashed arrows.

Basic theories for linking IVCT band shapes with the underlying electronic structure were developed by Mulliken[21] and extended by Hush.[22,23] These works were applied to mixed-valent systems, as classified by Robin and Day.[19] Information about the electronic coupling was extracted from the position and width of the IVCT band using the Mulliken–Hush treatment.[24] This initial treatment assumed a Gaussian-shaped band, although many real systems, including the CTI, exhibit an asymmetric IVCT band shape (Figure 1a–b). In order to resolve this discrepancy, alternative explanations for the shape of the IVCT band and, in turn, the interaction between the redox centres were introduced. Two approaches have been considered: (a) the IVCT band can either be reconstructed from the adiabatic potential energy curves, or (b) computed from a quantitative description of the interaction of diabatic states.

In the former case (a), the IVCT band is computed semi-classically[25,26] (i.e. the nuclear kinetic energy is neglected, and the vibrational levels are unknown) using the nuclear ensemble method[27] on the adiabatic potentials from the Marcus–Hush model.[1,2] These surfaces are drawn along an electron transfer coordinate (q, see Figure 1c), which is conceived of as an anti-symmetric motion involving the two redox sites of a mixed-valent system. One collects the excitation energies along this coordinate into an absorption band and weights them by the Boltzmann distribution on the ground state surface. However, because the vibrational levels are not included, the shape of the IVCT band cannot be reproduced if its origin is vibronic.

In the latter case (b), the IVCT band is obtained from a quantitative description of coupled diabatic states and the adiabatic states they produce.[11] A proper quantum mechanical description (including also the kinetic energy of the nuclei) can be achieved with vibronic coupling models.[28,29] A specific vibronic coupling model designed to describe the IVCT transition in the CTI was proposed by Piepho, Krausz and Schatz, the so-called PKS model.[10] The model has three parameters related to the postulated diabatic states, an interaction between the monomers (coupling term), a change of bond lengths upon oxidation/reduction, and the frequency of the totally symmetric stretch of the monomer. Because the diabatic states for a mixed valent system cannot be known exactly, they are approximated by an isolated monomeric unit. In the case of the CTI ion a logical choice is $[Ru(NH_3)_6]^{3+}$. The PKS approach proposes constructing the electron transfer coordinate as the anti-symmetric combination of the monomer stretches.

Hush[30,31] criticized the PKS model for its exclusion of a symmetric dimension. He expected the IVCT to involve an antibonding orbital of the bridge, producing a symmetric distortion of the bridge. As a consequence, the minimum of the IVCT state would be offset along a symmetric dimension, accounting for this distortion. Another point of criticism was that the anti-symmetric dimension was incompletely described by monomers, because it should also include vibrations of the bridging unit.

On the other hand, Ko and Ondrechen[12,32] reasoned that, in a two-state model, the symmetric dimension should remain decoupled from the electronic motion and not affect the absorption band shape. As an extension of the two-state model, they proposed to add a third diabatic state associated with the isolated bridge. This results in a three-mode three-state vibronic coupling model that is consistent with Hush's interpretation. It contains up to five parameters that need to be determined from spectroscopic data.[12,32]

An alternative idea by Reimers and Hush[11] was to introduce a two-state vibronic coupling model where the potential coupling depends linearly on the symmetric coordinate. This model accounts for multiple anti-symmetric and symmetric modes, however it was not yet possible to identify their precise nature and relation. In a similar fashion, the PKS model was later extended to account for multiple modes, including also the symmetric one.[33–35] These refinements adapted the vital features of the models proposed by Ko and Ondrechen[12] and addressed the criticism of Hush.[30,31]

All vibronic coupling models discussed above successfully describe the general IVCT band shape of the CTI, even though they build on different underlying assumptions.

Thus, it is difficult to identify which of the models best represents reality. Moreover, which normal modes contribute to electron transfer cannot be inferred from the model but needs to be postulated; it is challenging to postulate the correct weight for each of the normal modes. These points are important because the electronic structure implications differ widely, even up to the point of disagreeing whether the ground state has a single vs. double well potential.

We have recently proposed a method that quantitatively identifies the anti-symmetric dimension of intramolecular electron transfer according to the Marcus–Hush model from ab initio calculations.[36] The approach involves an ensemble generated from Wigner sampling at finite temperature, to which a multicomponent fit is applied that only assumes the validity of the Marcus–Hush model. The fitting procedure uses either the electron position or the IVCT energy as the descriptor for progress along the electron transfer coordinate. The anti-symmetric dimension for electron transfer is obtained as a linear combination using a basis of all vibrational modes.

Herein, we extend our approach to also identify the symmetric dimension, free of prior assumptions about the nature of electronic coupling. We find that the anti-symmetric dimension drives electron localization, while the minimum of the IVCT surface is offset with respect to the minimum of the ground state surface along the symmetric coordinate. We obtain the vibronic structure of the IVCT band from the adiabatic ab initio potentials spanned by only these two dimensions, thus achieving excellent agreement with the experimental shape of the band. Our approach is independent from the previously proposed vibronic coupling models as well as the semiclassical treatment. Despite this, our approach recovers the very surfaces that were sought by these prior models. We demonstrate our method using the CTI, but note it is likely general for systems with single welled potentials.

Results and Discussion

Electronic Structure

The Creutz–Taube ion,[3] (μ-pz)[$Ru^{II/III}(NH_3)_5$]$_2^{5+}$(pz = pyrazine), is a mixed-valent Class III complex in the nomenclature introduced by Robin and Day, i.e. fully delocalized.[19] The IVCT band of the CTI is centered around 6500 cm^{-1} and shows distinct asymmetry at the higher-energy side,[3] the origin of which has been assigned to vibronic transitions.[10,12,33,37] The IVCT band is solvent independent which is a marker for a delocalized electronic structure.[20,38,39]

As pointed out by Richardson and Taube,[40] the Ru atoms interact via superexchange as schematically shown in Figure 2. The in-phase and out-of-phase combinations of the Ru d_{xz} orbitals interact with the HOMO and LUMO of the pz bridge, which have one and two nodal planes perpendicular to the pz plane, respectively. Interaction with the LUMO produces the πd_{xz} orbital, in which the in-phase combination of the d-orbitals is stabilised. In contrast,

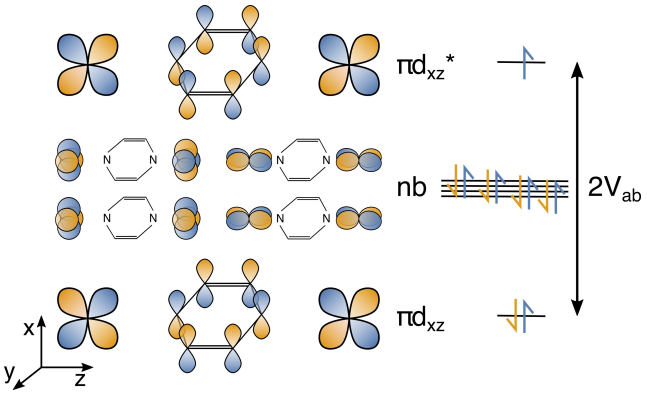

Figure 2. Molecular orbital diagram of the CTI depicting the interaction of the metal centers via the superexchange mechanism. The in-phase and out-of-phase combinations of the metal d_{xz} orbitals interact with the LUMO and HOMO of the pz bridge, respectively. The often used approximation to equate this orbital energy difference with $2V_{ab}$ is shown here.

interaction with the HOMO destabilises the out-of-phase combination of the d-orbitals and results in the πd_{xz}^* orbital, which is the SOMO of the Creutz–Taube ion.

Apart from the orbitals πd_{xz} and πd_{xz}^* that arise from superexchange, a set of four non-bonding orbitals are occupied in the frontier molecular orbital region. These essentially pure Ru d-orbitals participate in neither π- nor σ-bonding interactions with the pz bridge or the ammonia ligands. Excitations from these orbitals into the πd_{xz}^* orbitals will result in four electronic states that are lower in energy than the IVCT state. These states will, however, have transition dipole moments of zero.

While it is common to discuss the IVCT and the coupling strength in terms of transitions between πd_{xz} and πd_{xz}^* orbitals, this is not correct. Instead, the value $2V_{ab}$ in the Marcus–Hush model corresponds to the energy difference of the adiabatic electronic states. Calculating the potential coupling from the orbital energy difference does not lead to reliable absolute values because the Coulomb and exchange energy of the exciton are neglected.[41] Nevertheless, it is often convenient to discuss IVCT processes, energies and band shapes in terms of orbitals, with the caveat that it is, ultimately, the states they comprise that are of interest.

The vertical excitation energy to the IVCT state at the Franck–Condon point is 8516 cm^{-1} at the LH20t/def2-TZVP(def2-SVP) level of theory (as implemented in the TURBOMOLE package[42]), which has shown a great performance for mixed-valent compounds from the Class II/III borderline.[43] Given the high total charge of the complex, the agreement with the experimental value at 6500 cm^{-1} is satisfactory. However, such a simple calculation on a single geometry cannot provide any insight into the band shape. Using a nuclear ensemble approach, specifically Wigner sampling at 300 K, the IVCT band in implicit water solvation is predicted as a fairly symmetric, isolated absorption centered around 8500 cm^{-1}, see Figure 3a. The band is constructed from the individual excitations in Figure 3b, which almost exclusively have IVCT character, i.e. state D_5

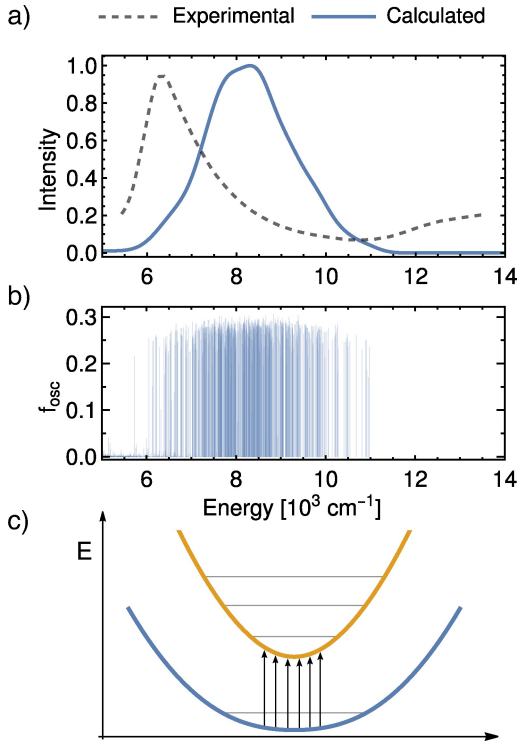

Figure 3. a) Experimental and calculated spectrum using 600 single point calculations (LH20t/def2-TZVP) from Wigner sampling. The experimental spectrum is reproduced from Ref. [3] with permission. b) The oscillator strengths from the individual single point calculations. c) Schematic description of the nuclear ensemble approach.

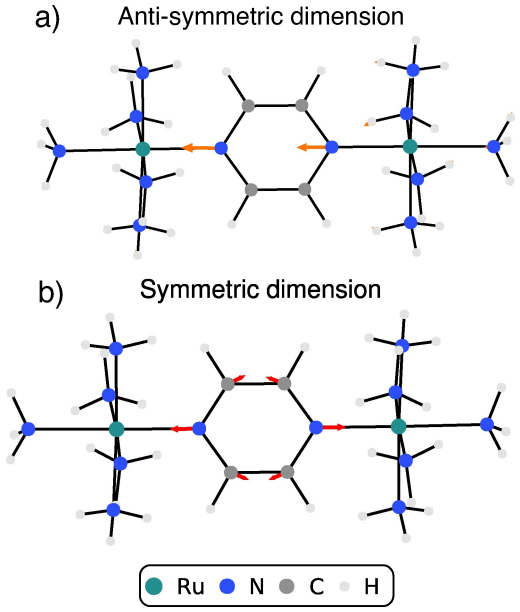

Figure 4. a) Marcus dimension of electron transfer obtained by fitting to the electron position in the ensemble. b) Symmetric dimension obtained by fitting to the excitation energy of the IVCT state.

is dominated by transitions of type $\pi d_{xz} \rightarrow \pi d^*_{xz}$. In comparison with the experimental spectrum, the IVCT band shape calculated in this way appears too symmetric and too broad. Thus, even though the nuclear ensemble approach accounts for the full dimensionality of the system and adds vibrational resolution to the electronic absorption band, it fails to reproduce the correct shape. A central reason is that all the Franck–Condon factors are set to 1 in this methodology, i.e. the vibrational levels are ignored as shown in Figure 3c.[27] A correct treatment requires the calculation of the proper vibronic structure, but this requires knowledge of the dimensions relevant for the IVCT process.

Marcus Dimensions: Anti-Symmetric and Symmetric Motions

Access to a correct treatment of the Franck–Condon factors requires that the PES along the dimensions relevant to the IVCT process be known. The anti-symmetric motion of the CTI is identified as isolated, unidirectional movements of the pz bridge nitrogen atoms along the Ru–Ru axis, see Figure 4a, using our recently established procedure.[36] This finding is consistent with the superexchange mechanism (Figure 2): for positive displacements, the interaction of the pz bridge is strengthened with the Ru atom on the left and weakened with the Ru atom on the right, which should lead to electron localization. The normal mode contributions to the anti-symmetric dimension (Huang–Rhys factors) are shown in Figure 5a. This decomposition into normal modes allows for a straightforward calculation of the reorganization energy[44] even for a fully delocalized system. We found a value of 8612 cm^{-1} (see Table 1). Comparison with the calculated value of the potential coupling $2V_{ab} = 8515$ cm^{-1}, using the excitation energy at the Franck–Condon geometry, sets the CTI to the Class II/III borderline, i.e. to the borderline of localized and delocalized electronic structure. We note that this is in agreement with the experimental literature, where it has been repeatedly shown that the CTI is situated near the Class II/III border.[4]

Besides the anti-symmetric motion, a symmetric dimension has been invoked to explain the properties of mixed-valent compounds. According to Hush,[30] the minima of the ground and the IVCT states should not be perfectly nested since the IVCT process describes an excitation to an orbital with greater antibonding character, which will result in a symmetrical distortion of the molecule. This argument can be exploited to identify and quantify the symmetric dimension. Fitting the normal coordinates to the IVCT

Table 1: Properties of the identified dimensions. The reorganization energy was computed from the Huang–Rhys factors as: $\lambda = \sum_i S_i \hbar\omega_i$. The ZPE is the energy of a relaxed wave packet in the one-dimensional potential along the respective dimension. The potentials are presented in Figure 6a–b and further computational details are given in the SI.

	anti-symmetric	symmetric
λ [cm^{-1}]	8612	4139
ZPE [cm^{-1}]	534	634
mass [amu]	13.0081	15.6780

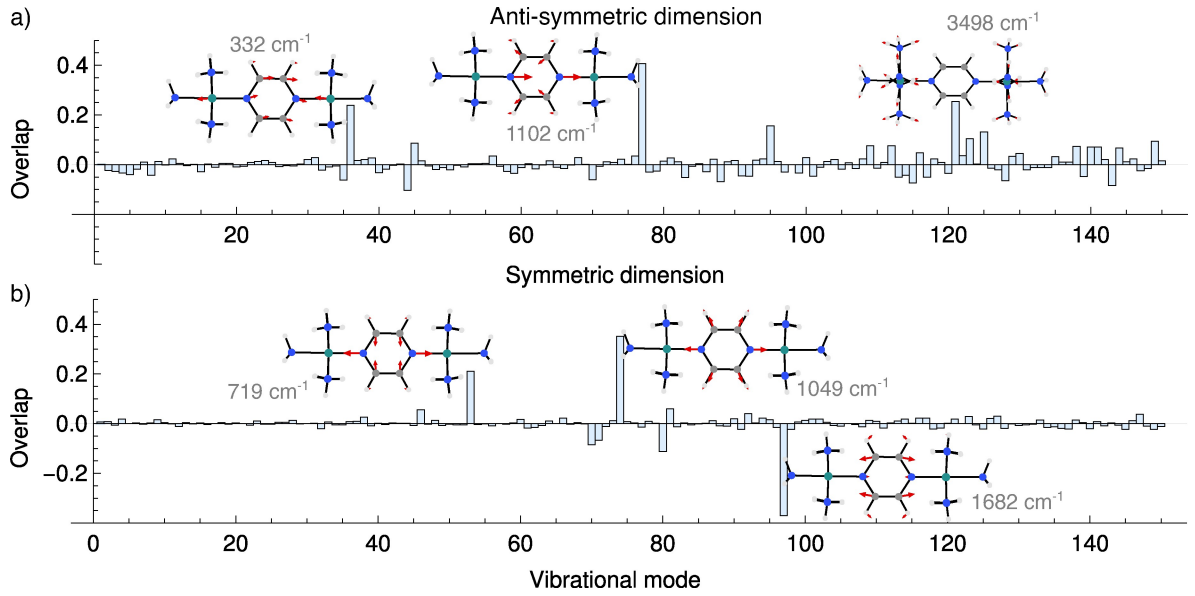

Figure 5. Calculated Huang–Rhys factors as a projection of normal modes to the anti-symmetric (panel a) and symmetric (panel b) dimensions. The dominant contributors are depicted as insets along with the respective frequencies.

excitation energy identifies the dimension along which the minima of the ground and excited state potentials are offset, ignoring dimensions along which they are not.[36]

The symmetric dimension we find in this way is confined exclusively to the pz bridge and modulates the Ru–pz distances as well as the N–C and C–C interactions, see Figure 4b. It is essentially orthogonal to the anti-symmetric dimension (overlap of 0.057). Three normal modes dominate the contribution to this symmetric dimension, Figure 5b, all of which are symmetric stretches of the pz bridge. These findings confirm Hush's argument:[11,30,31] a symmetric dimension exists that contains vibrations of the bridge, and along which the minimum of the IVCT potential energy surface is offset with respect to the ground state potential.

In Table 1 we summarize the key parameters of the identified dimensions. The reorganization energy for the symmetric dimension does not have a clear interpretation in the scope of the Marcus–Hush model, but it is computed for completeness. The different ZPEs imply only slightly different curvatures of the ground state potentials along the two dimensions. Additional information can be extracted from the normal mode masses of the dimensions. For the anti-symmetric dimension, the value is lower than the mass of a nitrogen atom which suggests that lighter atoms must participate. Indeed, a close inspection of the motion in Figure 4a (top right) shows the participation of hydrogen atoms. Since these contributions are small in magnitude and asymmetric, we suspect that they are due to noise in the ensemble. In the symmetric dimension, the mass is higher than the mass of a nitrogen atom. This is caused by the participation of the ruthenium atoms, but their contribution is too small to be visible in Figure 4b. It is thus difficult to determine whether or not their contribution originates from a noisy ensemble. Nevertheless, the dimensions we identify clearly match chemical expectations, and hence they are suitable for evaluating the potential energy surfaces of the electronic states.

1D Potentials for Anti-Symmetric and Symmetric Dimensions

Predicting the vibronic contributions to the IVCT band requires that the relevant potentials be known. A scan along the anti-symmetric dimension reveals the expected Class III behavior (Figure 6a), i.e. the ground and the IVCT states are nested and have single minima. The four states D_{1-4} characterized by excitations from non-bonding orbitals to the SOMO (see Figure 2) exhibit a second-order Jahn–Teller effect at the Franck–Condon point (position 0.0 Å). They are, however, not relevant for the discussion of the mixed-valence behaviour of the CTI because of their energy separation from both the ground and the IVCT states. The chemically relevant spatial extent of the anti-symmetric dimension is very narrow, suggesting a higher frequency motion than usually assumed. The fundamental frequency employed in the vibronic coupling models is usually around 500 cm^{-1}, corresponding to a ZPE of 250 cm^{-1} for a harmonic oscillator.[10,33] We find a significantly higher zero-point energy of 534 cm^{-1} again suggesting a higher frequency motion (see Table 1). The reason that underestimated frequencies have been used in past vibronic coupling treatments is that modes were chosen by inspection of vibrational spectra. Since the participation of low-frequency skeletal modes is chemically intuitive, their contribution may have been overweighted. Our approach identifies and weights all relevant modes from ab initio calculations, avoiding bias against high frequency modes.

A scan along the symmetric coordinate (Figure 6b) shows that the minimum of the IVCT state is shifted towards negative displacements (i.e. upon a contraction of the pz

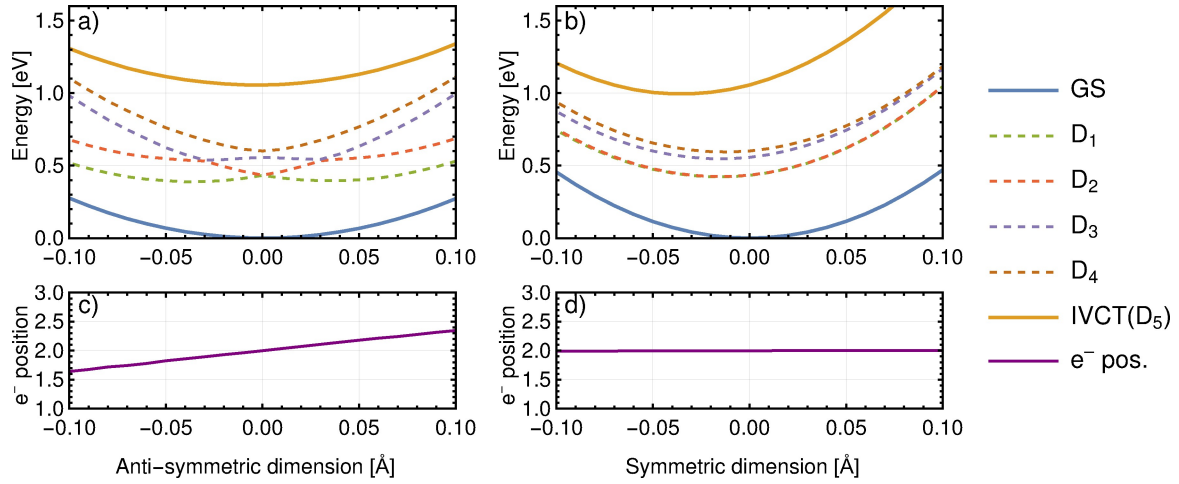

Figure 6. One dimensional scans along (a) anti-symmetric and (b) symmetric dimensions depicting the potential energy curves of the six lowest electronic states. The electron position as a measure of the degree of localization is plotted in panels (c) and (d) for the anti-symmetric and symmetric dimensions, respectively. The scans were performed with a step size of 0.01 Å.

bridge) relative to the ground state. Similarly to the anti-symmetric dimension, the symmetric one appears to be a high frequency motion which is confirmed by the calculated zero-point energy of 643 cm^{-1} (see Table 1). The offset of the IVCT potential will have an impact on the shape of the absorption band, especially if the energy spacing of the vibrational levels is large.

The electron transfer process is usually assumed to occur along only one coordinate, assigned to the anti-symmetric coordinate. Therefore, it should be verified that electron localisation occurs only along one of the dimensions we identified. The degree of electron localization in the ground state is depicted in Figure 6c. A value of 1 would mean a complete localization of the unpaired electron at one $[Ru(NH_3)_5]^{2+/3+}$ unit, and equivalently a value of 3 would mean a complete localization on the other unit. Starting from the Franck–Condon point, movement of the atoms along the anti-symmetric dimension leads to a localization of the unpaired electron on the Ru ions. In the scope of the Marcus–Hush model, such a localization corresponds to a change in the admixture of the diabatic state comprising the adiabatic one. In contrast, movement along the symmetric dimension reveals no change in the degree of electron localization, Figure 6d. Thus the dimensions we find with our ab initio procedure satisfy all formal requirements expected of the electron transfer coordinates postulated in the Marcus–Hush model.

2D Potentials from Anti-Symmetric and Symmetric Dimensions

To construct the PES spanned by the anti-symmetric and symmetric dimensions, we performed a two dimensional scan, see Figure 7a–b. With the dimensions now being quantified in spatial units, a direct comparison between the two coordinates is possible for the first time. The ground state potential energy surface of the CTI, Figure 7a, is steeper along the symmetric dimension. This finding is consistent with the assumption commonly made for the two-dimensional two-state Marcus–Hush model, where the potential along the anti-symmetric dimension is expected to be flatter due to the merged minima of the diabatic basis.

The potential of the IVCT state is plotted in Figure 7b. It has a single minimum and it is again steeper in the symmetric dimension with an apparent degree of anharmonicity (more clearly visible in Figure 6b). An important feature is the offset of the minimum with respect to the ground state along the symmetric coordinate. The traditional two-state model,[1,45] even in two dimensions, provides no means to incorporate an offset along the symmetric dimension. There are two possible extensions of the model that could allow such an offset:

I) A third diabatic state shifted along the symmetric dimension could be introduced. This state is usually labelled as the bridge state.[12,25] However, if the bridge state were responsible for the offset of the minima, we should be able to find an adiabatic state with a large contribution of metal-to-bride charge transfer (MBCT) character close to the near infra-red region. The energetically closest MBCT state is situated at about 1.4 eV above the IVCT state (see SI), so that its influence on the other states is expected to be extremely limited. We therefore find this explanation implausible.

II) Geometry dependent coupling between the diabatic basis in the two-dimensional two-state Marcus–Hush model could arise because movement along the symmetric coordinate will result in a change in the Ru–bridge distance, hence altering the coupling strength. An increase in coupling by moving along only the symmetric dimension in one direction will push the adiabats apart, while a decrease in coupling by movement in the other direction will bring them closer together, as illustrated in Figure 7e. This must result in an offset of the minima. The coupling strength along the anti-symmetric dimension remains unaffected as depicted in Figure 7d. This explanation appears reasonable in the context of the

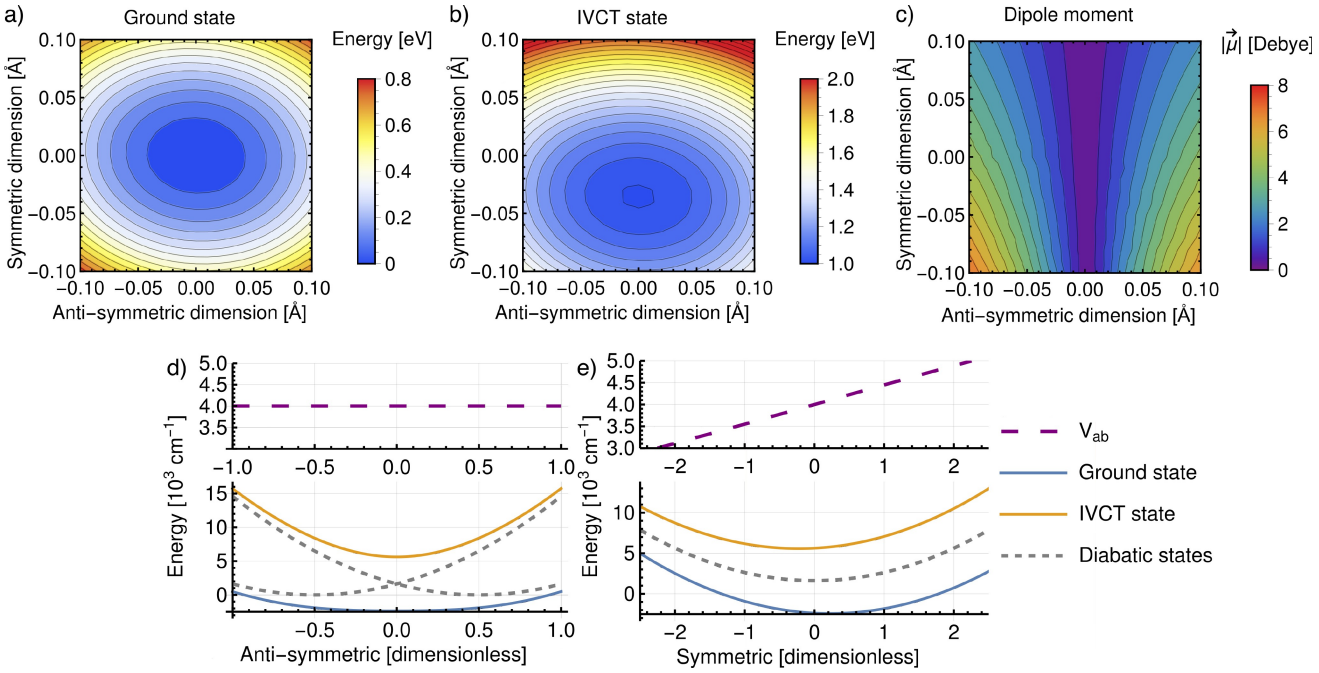

Figure 7. Two dimensional scans along the anti-symmetric and symmetric dimensions. a–b) Two dimensional potential energy surfaces of the ground and IVCT states, respectively. c) Two dimensional distribution of the dipole moment in the ground electronic state. The scans were performed in a range of displacements from −0.16 to 0.16 Å in both dimensions with a step size of 0.01 Å. d–e) One-dimensional cuts of the analytical Marcus–Hush model with two states, two dimensions and geometry dependent coupling. Cuts are created by setting one of the coordinates to zero. A more detailed description is given in the SI.

dimensions we identified, and is in accord with the superexchange coupling mechanism.[40] This situation would be consistent with the point of view of Reimers and Hush,[11] but only restricted to a single anti-symmetric and symmetric mode. The geometry dependent coupling is a natural result of the vibrational motion of the complex, but it remains to be seen to what extent it can explain our observations. We will explore this idea below.

Though we could continue to use the electron position to monitor the electron localization, as in Figure 6c–d, the dipole moment is just as valid, while being experimentally more accessible. Distribution of the dipole moment in the two-dimensional scan produces Figure 7c. Starting from any point, any displacement (both positive and negative) along the anti-symmetric dimension leads to a change in localization of the unpaired electron and, consequently, to a change in the dipole moment magnitude. In contrast, there is a single line parallel to the symmetric dimension and passing through the origin along which the dipole moment does not change (i.e. will remain zero). Starting from any other displacement along the anti-symmetric dimension and moving along the symmetric dimension will result in a change in dipole moment. The two-state two-dimensional Marcus–Hush model cannot explain this behaviour, where the composition of the diabatic states in the adiabatic ground state (which can be directly connected to the dipole moment and the electron position) remains constant along the symmetric dimension under all circumstances. In contrast, extending the Marcus–Hush model by introducing a dependence of the coupling on the position along the symmetric dimension explains this behaviour. Details on this modified Marcus–Hush model are given in analytical form in the SI.

Since the dipole moment can change along the symmetric dimension, the symmetric mode may become detectable in the IR spectrum through anharmonic and non-Condon effects. In fact, IR-active symmetric modes have been observed in several mixed valence systems, but no satisfactory explanation has emerged.[46,47] In our analysis of the two-dimensional scanned potential, the vibrational transition that would correspond to the excitation in the symmetric dimension (1392 cm^{-1}) is weaker by a factor of 100 than the transition in the anti-symmetric dimension (973 cm^{-1}; details in the SI). Thus, our ab initio data in their current form do not explain the experimental observation. However, considering environmental effects explicitly may change this.

IVCT Band Shapes

We will use the calculated one- and two-dimensional potential energy surfaces (Figures 6a–b, 7a–b) to reconstruct the IVCT absorption band shape. To this end, two approaches are used: a nuclear ensemble approach and wave packet (WP) dynamics. Technical details are provided in the SI. Within the nuclear ensemble approach, the spectrum is calculated as a distribution of energy differences between the ground and IVCT states weighted by the

respective Boltzmann probabilities. The approach is semi-classical and the vibronic transitions are not accessible, Figure 8c. With WP dynamics, the spectrum is computed as a Fourier transform of an autocorrelation function which is obtained by numerical propagation of a ground state-relaxed WP on the IVCT potential surface. In this way, the vibronic structure of the absorption band is fully recovered, Figure 8f.

Advantages of utilizing adiabatic potentials from ab initio calculations are that the calculation of spectra is free of any pre-postulated parameters, and that the energy differences and curvatures of the potentials reflect those of the real system according to the chosen level of theory. The resulting spectra will naturally depend on the choice of coordinates spanning the potential. In our approach, no system-specific assumptions about the coordinate(s) were made: the only requirement is that each coordinate satisfy a given property of the Marcus–Hush model, i.e. moving from the ground state minimum either involves electron localization (anti-symmetric) or an offset of the potential energy surfaces (symmetric).

Focusing first on the spectra computed with the nuclear ensemble method, Figure 8a–b, the asymmetry of the experimental band shape is severely underestimated. Furthermore, the computed spectrum utilizing only the anti-symmetric dimension (Figure 8a) is very narrow. This may be surprising at first glance because it has been repeatedly demonstrated that the two nested adiabats with different curvatures are responsible for the asymmetric band shape according to the Marcus–Hush model.[25,26] Inspecting the ab initio potentials presented in Figure 8a reveals that they have almost identical curvatures, which explains the absence of asymmetry in the calculated spectrum. Accounting for both dimensions, Figure 8b, leads to a small degree of asymmetry. However, the computed spectrum still misses the long high-energy tail. Overall, the nuclear ensemble approach thus fails to reproduce the experimental IVCT band shape.

Accounting for the proper vibronic structure of the IVCT band by using WP dynamics, Figure 8d–e, leads to a similarly narrow shape when considering only the anti-symmetric dimension (Figure 8d). The spectrum contains only one vibronic transition between the vibrational ground states of the ground and IVCT potentials; the vibronic transitions to higher vibrational states are missing. This is due to the perfect nesting of the two potentials and their almost identical curvatures in the anti-symmetric dimension. While the former is in perfect agreement with the Marcus–Hush model, the latter diverges from the model. Nearly identical curvatures of the ground and IVCT states would be possible only for large couplings ($2V_{ab} \gg \lambda$). However, the coupling strength and the reorganization energy computed here set the CTI to the Class II/III borderline ($2V_{ab} \approx \lambda$). This deviation from the conceptual model can be expected since we do not rely on the existence of a harmonic diabatic basis.

When accounting for both dimensions (Figure 8e), the IVCT band has the correct width and a clearly asymmetric shape. There are three vibronic transitions separated by approximately 1500 cm^{-1}. This is consistent with the high curvatures of the PESs, which can, in turn, explain the insufficient description of the IVCT band with the nuclear ensemble approach (panel b): because the zero-point energy is neglected in the nuclear ensemble approach, a smaller

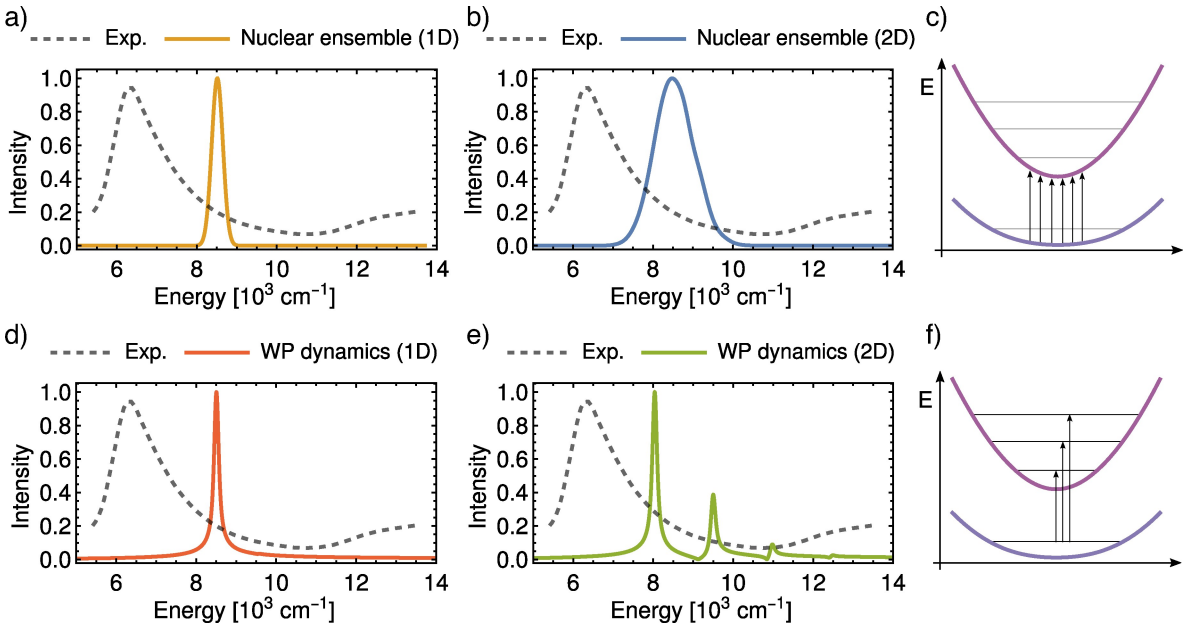

Figure 8. IVCT spectra obtained from one-dimensional or two-dimensional scans along the anti-symmetric dimension. a–b) Spectra computed with the nuclear ensemble approach from one- and two-dimensional PESs, respectively. c) Computed transitions via nuclear ensemble approach. d–e) Spectra computed using the Fourier transform of an auto-correlation function from wave packet dynamics on one- and two-dimensional PESs, respectively. f) Computed transitions via WP dynamics. The experimental spectrum is reproduced from Ref. [3] with permission.

portion of the coordinate space is accessible and hence the absorption band will be too narrow. Importantly, the second and third vibronic transitions gain intensity because of the offset potentials in the symmetric dimension. We note that further refinements of the WP dynamics results, e.g. regarding broadening or position of the IVCT band with respect to experiment, can presumably be achieved by including the solvent-induced changes of the PESs or going beyond the Condon approximation.

In conclusion, the correct shape and width of the IVCT band can be reconstructed only when the proper vibronic structure is taken into account and the minima of the PESs are offset in the symmetric dimension. Our findings support the proposal of Reimers and Hush[11] that the symmetric dimension is of high importance for delocalized systems like the CTI, and contradict the conclusion of Piepho[33] that the high energy tail of the IVCT band is unlikely to be associated with the symmetric modes. The offset potentials can be reconciled within the Marcus–Hush model by introducing geometry dependent coupling, as elaborated in detail in the following section.

Geometry Dependent Coupling

Throughout this work, we have aimed to connect ab initio data to the Marcus–Hush model. By inspection of the predicted IVCT absorption bands, we concluded that a model with two states and one dimension is not sufficient to capture all electronic and vibrational aspects of the molecule that give rise to the position and shape of the IVCT band. We demonstrated that an additional symmetric dimension is an *intrinsic* feature of bridged systems, and that the potential coupling between the metal centers V_{ab} has to depend on this dimension. We can confidently state at this point that two dimensions and two states with geometry dependent coupling are necessary to discuss the properties of the CTI. In the following, we explain the origin of this effect.

The geometry dependence of the coupling is rooted in the superexchange mechanism (Figure 9), which conceptualises how the interaction between the redox centers is mediated via the molecular bridge. As is shown in the MO diagram in Figure 2, the in-phase and out-of-phase combinations of the metal d_{xz} orbitals interact with the π-type HOMO and π*-type LUMO of the pyrazine bridge, respectively.[40] To simplify the discussion of geometry dependent coupling, we represent the pyrazine bridge by a diatomic bridge. Figure 9a shows the expected MOs for the equilibrium configuration. The bonding interaction between the in-phase combination of the d_{xz} orbitals with the LUMO of the bridge produces an MO that is lower in energy than the MO formed by the antibonding combination of the out-of-phase d_{xz} orbitals and the HOMO of the bridge. The latter becomes the SOMO of the mixed valence state, while the other is doubly occupied. The energy difference between the newly formed frontier molecular orbitals can be used as a first approximation for twice the potential coupling value, $2V_{ab}$. With the MO diagram for the equilibrium structure in hand, we now discuss the influence of the anti-symmetric and the symmetric motion on the molecular orbitals and thereby on the potential coupling.

In Figure 9b, the anti-symmetric dimension is represented by a distortion of the molecule in which both bridging atoms move in the same direction. This movement will increase the orbital overlap with one metal center and simultaneously decrease the overlap with the other metal center. Since these effects oppose one another, the energy splitting of the frontier MOs, and in turn $2V_{ab}$, remains largely unchanged. This picture of a constant potential coupling corresponds to the expectations set by the one-dimensional two-state Marcus–Hush model and its extensions.[25]

The symmetric dimension is represented by the movement of only the bridging atoms towards one another (Figure 9c, negative direction) and away from each other (Figure 9d, positive direction). Contraction of the bridge as in Figure 9c leads to a decreased overlap of the bridge orbitals with the metal d-orbitals. This decreases the energy gap between doubly and singly occupied molecular orbitals, resulting in a smaller V_{ab}. For a distortion in the positive direction (Figure 9d), the situation is exactly the opposite: expansion of the bridge leads to a larger overlap with the d-

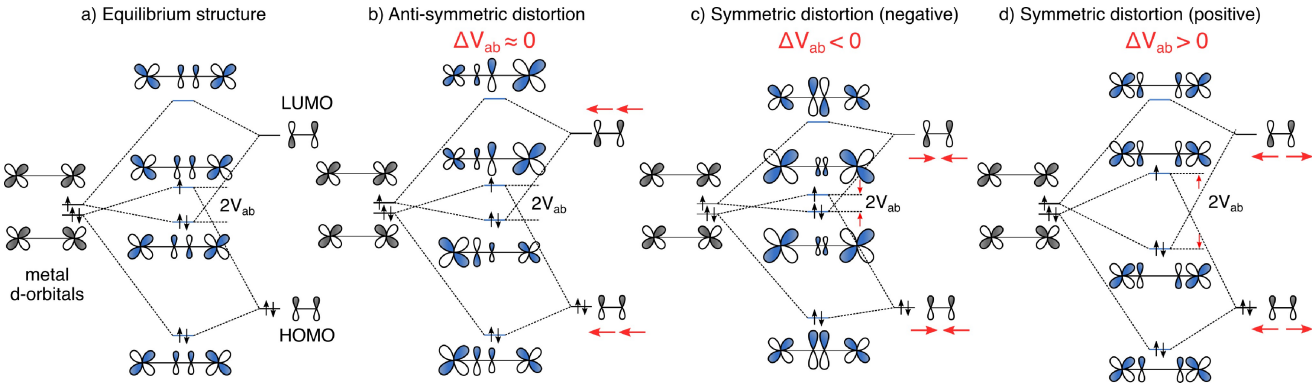

Figure 9. Schematic description of the effects of symmetric and anti-symmetric distortions on the potential coupling between the metal centers within the superexchange mechanism. a) Equilibrium configuration. b) Anti-symmetric distortion is realized by moving the bridge towards one metal center. c–d) Negative and positive symmetric distortions are realized as contraction and expansion of the bridge, respectively.

orbitals, thus a larger energy gap, and as a result an increased coupling strength (V_{ab}). These simple MO considerations demonstrate that motion along the symmetric dimension must affect the magnitude of coupling V_{ab}.

A simplified way of monitoring this dependence in the ab initio scans is provided with the energy difference of the frontier orbitals, see Figure 10a–b. The true coupling refers to the energy difference of the respective states at the Franck–Condon point, and the pure Marcus–Hush model provides no access to variations of V_{ab} beyond the equilibrium structure. A visualisation of the variance in V_{ab} along the symmetric and anti-symmetric dimensions is shown in Figure 10c. The absolute values of V_{ab} shown here are twice as large as expected from the position of the IVCT band and the excitation energy at the Franck–Condon point, largely due to neglecting the Coulomb and exchange energy of the exciton. Nevertheless, the qualitative trends demonstrate the extent of geometry dependent coupling as a function of the two relevant dimensions.

Along the anti-symmetric dimension, the change in the V_{ab} is almost negligible. In contrast, V_{ab} changes significantly along the symmetric dimension (approximately by 40 %). These findings confirm the conceptual understanding of the superexchange mechanism discussed above. Furthermore, they explain the observed change in dipole moment along the symmetric dimension, the offset of the minima of the ground and IVCT states, and the asymmetric shape of the IVCT band.

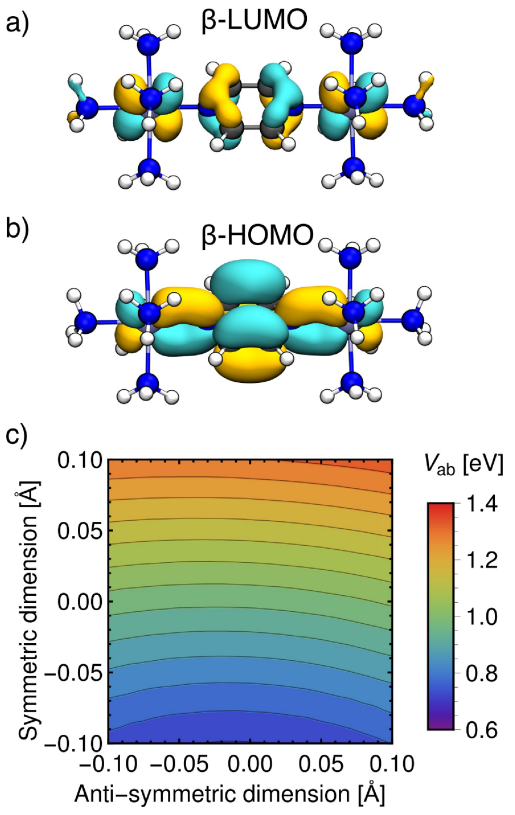

Figure 10. Geometry dependence of potential coupling V_{ab}. a) β-LUMO; b) β-HOMO; c) Two-dimensional dependence of V_{ab} on anti-symmetric and symmetric dimension. V_{ab} is computed as $(\varepsilon(\text{LUMO})-\varepsilon(\text{HOMO}))/2$.

Conclusion

While an anti-symmetric dimension is present in all descriptions of ET, we have shown here that, additionally, a symmetric dimension is intrinsic to and required for accurate descriptions of bridged systems. We provided an approach for identifying and quantifying this symmetric dimension from ab initio calculations. It is constructed as a linear combination of normal modes, in a complementary manner to our approach for quantifying the anti-symmetric dimension.[36] Our method reaches the same objective as the vibronic coupling models, but relies only on ab initio calculations rather than pre-postulated diabatic states. This resolves the decades-old question of which coordinate(s) are required to explain the IVCT band of strongly coupled bridged systems, as showcased here using the Creutz–Taube ion.

An advantage of our approach is that we can for the first time explain the shape of the IVCT band using the exact required dimensions and associated potentials from ab initio calculations. We have shown that to capture the characteristic high-energy tail of the IVCT band, the vibronic transitions between the potentials spanned by these two dimensions are needed. These arise from the offset minima of the ground state and excited state potentials in the direction of the symmetric dimension. This offset is a result of geometry dependent coupling along the symmetric dimension which must be a natural consequence of the well-known superexchange mechanism.

Though we are providing a new ab initio route for rationalising mixed-valent electron transfer systems, we can connect the results with the established models and their specific parameters. For instance, we can recover the potential coupling and the reorganization energy even for fully delocalized systems. Our method is easily accessible and widely applicable. Potential application areas include enzymatic electron transfer, (electro-)catalysis, photosensitizer chemistry, molecular electronics and superconductivity.

Acknowledgements

The authors thank Peter Vöhringer for insightful discussions on wave packet dynamics. A.S. thanks the Merck'sche Gesellschaft für Kunst und Wissenschaft e.V. for financial support. The authors gratefully acknowledge the computing time provided to them on the high-performance computer Lichtenberg at the NHR Centers NHR4CES at TU Darmstadt. This is funded by the Federal Ministry of Education and Research, and the state governments participating on the basis of the resolutions of the GWK for national high performance computing at universities.

Acknowledgements

Open Access funding enabled and organized by Projekt DEAL.

Conflict of Interest

There are no conflicts of interest to declare.

Data Availability Statement

The data that support the findings of this study are available in the supplementary material of this article.

Keywords: electron transfer · mixed-valent chemistry · quantum chemistry · nuclear dimensions · spectroscopy

[1] R. A. Marcus, *J. Chem. Phys.* **1956**, *24*, 966.
[2] N. S. Hush, *Trans. Faraday Soc.* **1961**, *57*, 557.
[3] C. Creutz, H. Taube, *J. Am. Chem. Soc.* **1969**, *91*, 3988.
[4] C. Creutz, Mixed Valence Complexes of d5-d6 *Metal Centers, in Progress in Inorganic Chemistry*, pages 1–73, John Wiley & Sons, Ltd **1983**.
[5] U. Fuerholz, H. B. Buergi, F. E. Wagner, A. Stebler, J. H. Ammeter, E. Krausz, R. J. H. Clark, M. J. Stead, A. Ludi, *J. Am. Chem. Soc.* **1984**, *106*, 121.
[6] S. P. Best, R. J. H. Clark, R. C. S. McQueen, S. Joss, *J. Am. Chem. Soc.* **1989**, *111*, 548.
[7] P. A. Lay, R. H. Magnuson, H. Taube, *Inorg. Chem.* **1988**, *27*, 2364.
[8] W. Kaim, A. Klein, M. Glöckle, *Acc. Chem. Res.* **2000**, *33*, 755.
[9] G. E. Pieslinger, I. Ramírez-Wierzbicki, A. Cadranel, *Angew. Chem. Int. Ed.* **2022**, *61*.
[10] S. B. Piepho, E. R. Krausz, P. N. Schatz, *J. Am. Chem. Soc.* **1978**, *100*, 2996.
[11] J. Reimers, N. Hush, *Chem. Phys.* **1996**, *208*, 177.
[12] J. Ko, M. J. Ondrechen, *J. Am. Chem. Soc.* **1985**, *107*, 6161.
[13] A. Bencini, I. Ciofini, C. A. Daul, A. Ferretti, *J. Am. Chem. Soc.* **1999**, *121*, 11418.
[14] M. Parthey, M. Kaupp, *Chem. Soc. Rev.* **2014**, *43*, 5067.
[15] J. W. Lauher, *Inorg. Chim. Acta* **1980**, *39*, 119.
[16] H. Bolvin, *Inorg. Chem.* **2007**, *46*, 417.
[17] M. Parthey, J. B. G. Gluyas, M. A. Fox, P. J. Low, M. Kaupp, *Chem. - Eur. J.* **2014**, *20*, 6895.
[18] A. Šrut, V. Krewald, *J. Phys. Chem. A* **2023**, *127*, 9911.
[19] M. B. Robin, P. Day, *Mixed Valence Chemistry – A Survey and Classification*, vol. 10, pages 247–422, Academic Press **1968**.
[20] K. D. Demadis, C. M. Hartshorn, T. J. Meyer, *Chem. Rev.* **2001**, *101*, 2655.
[21] R. S. Mulliken, *J. Am. Chem. Soc.* **1952**, *74*, 811.
[22] N. S. Hush, *Intervalence-Transfer Absorption. Part 2. Theoretical Considerations and Spectroscopic Data*, pages 391–444, John Wiley & Sons, Ltd **1967**.
[23] N. S. Hush, *Electrochim. Acta* **1968**, *13*, 1005.
[24] C. Creutz, M. D. Newton, N. Sutin, *J. Photochem. Photobiol. A* **1994**, *82*, 47.
[25] B. S. Brunschwig, C. Creutz, N. Sutin, *Chem. Soc. Rev.* **2002**, *31*, 168.
[26] A. Heckmann, C. Lambert, *Angew. Chem. Int. Ed.* **2012**, *51*, 326.
[27] R. Crespo-Otero, M. Barbatti, *Theor. Chem. Acc.* **2012**, *131*, 1.
[28] R. L. Fulton, M. Gouterman, *J. Chem. Phys.* **1961**, *35*, 1059.
[29] I. B. Bersuker, *Chem. Rev.* **2021**, *121*, 1463.
[30] N. S. Hush, *Electron Delocalization, Structure and Dynamics in Mixed-Valence Systems*, pages 151–188, Springer Netherlands, Dordrecht **1980**.
[31] N. S. Hush, *Parameters of Electron-Transfer Kinetics*, chapter 13, pages 301–332, ACS **1982**.
[32] J. Ko, M. J. Ondrechen, *Chem. Phys. Lett.* **1984**, *112*, 507.
[33] S. B. Piepho, *J. Am. Chem. Soc.* **1990**, *112*, 4197.
[34] S. B. Piepho, *J. Am. Chem. Soc.* **1988**, *110*, 6319.
[35] P. N. Schatz, *Vibronic Coupling Models of Mixed Valency: Relation of the PKS and MO Models for One- and Two-Electron Systems*, pages 7–28, Springer Netherlands, Dordrecht **1991**.
[36] A. Šrut, B. J. Lear, V. Krewald, *Chem. Sci.* **2023**, *14*, 9213.
[37] M. J. Ondrechen, J. Ko, L. T. Zhang, *J. Am. Chem. Soc.* **1987**, *109*, 1672.
[38] B. J. Lear, S. D. Glover, J. C. Salsman, C. H. Londergan, C. P. Kubiak, *J. Am. Chem. Soc.* **2007**, *129*, 12772.
[39] C. Creutz, M. H. Chou, *Inorg. Chem.* **1987**, *26*, 2995.
[40] D. E. Richardson, H. Taube, *J. Am. Chem. Soc.* **1983**, *105*, 40.
[41] P. Kimber, F. Plasser, *Phys. Chem. Chem. Phys.* **2020**, *22*, 6058.
[42] S. G. Balasubramani, G. P. Chen, S. Coriani, M. Diedenhofen, M. S. Frank, Y. J. Franzke, F. Furche, R. Grotjahn, M. E. Harding, C. Hättig, A. Hellweg, B. Helmich-Paris, C. Holzer, U. Huniar, M. Kaupp, A. Marefat Khah, S. Karbalaei Khani, T. Müller, F. Mack, B. D. Nguyen, S. M. Parker, E. Perlt, D. Rappoport, K. Reiter, S. Roy, M. Rückert, G. Schmitz, M. Sierka, E. Tapavicza, D. P. Tew, C. van Wüllen, V. K. Voora, F. Weigend, A. Wodyński, J. M. Yu, *J. Chem. Phys.* **2020**, *152*, 184107.
[43] M. Haasler, T. M. Maier, R. Grotjahn, S. Gückel, A. V. Arbuznikov, M. Kaupp, *J. Chem. Theory Comput.* **2020**, *16*, 5645.
[44] C.-P. Hsu, *Phys. Chem. Chem. Phys.* **2020**, *22*, 21630.
[45] N. S. Hush, *Coord. Chem. Rev.* **1985**, *64*, 135.
[46] C. H. Londergan, J. C. Salsman, S. Ronco, C. P. Kubiak, *Inorg. Chem.* **2003**, *42*, 926.
[47] R. C. Rocha, A. P. Shreve, *Chem. Phys.* **2006**, *326*, 24.

Manuscript received: March 8, 2024
Version of record online: July 1, 2024